Title

The Lung Microenvironment Instructs Gene Transcription in Neonatal and Adult Alveolar Macrophages.

Journal

The Journal of Immunology, 208(8)

ISSN

0022-1767

Authors

Honda, Asami
Hoeksema, Marten A
Sakai, Mashito
et al.

Publication Date

2022-04-15

DOI

10.4049/jimmunol.2101192

Peer reviewed

HHS Public Access

Author manuscript

J Immunol. Author manuscript; available in PMC 2023 April 15.

Published in final edited form as:

J Immunol. 2022 April 15; 208(8): 1947–1959. doi:10.4049/jimmunol.2101192.

The Lung Microenvironment Instructs Gene Transcription in Neonatal and Adult Alveolar Macrophages

Asami Honda[*], **Marten A. Hoeksema**[†], **Mashito Sakai**[†], **Sean J. Lund**[*], **Omar Lakhdari**[*], **Lindsay D. Butcher**[‡], **Tara C. Rambaldo**[§], **Neal M. Sekiya**[§], **Chanond A. Nasamran**[¶], **Kathleen M. Fisch**[¶,||], **Eniko Sajti**[*], **Christopher K. Glass**[†,#], **Lawrence S. Prince**[‡]

[*]Department of Pediatrics, University of California San Diego, La Jolla, CA; Rady Children's Hospital, San Diego, CA

[†]Department of Cellular and Molecular Medicine, University of California, San Diego, La Jolla, CA

[‡]Department of Pediatrics, Stanford University School of Medicine, Palo Alto, CA

[§]San Diego Center for AIDS Research, San Diego, CA

[¶]Center for Computational Biology & Bioinformatics, University of California, San Diego, La Jolla, CA

[||]Department of Obstetrics, Gynecology & Reproductive Sciences, University of California, San Diego, La Jolla, CA

[#]Department of Medicine, University of California, San Diego, La Jolla, CA

Abstract

Immaturity of alveolar macrophages (AMs) around birth contributes to the susceptibility of newborns to lung disease. However, the molecular features differentiating neonatal and mature, adult AMs are poorly understood. Here we identify the unique transcriptomes and enhancer landscapes of neonatal and adult AMs in mice. While the core AM signature was similar, murine adult AMs expressed higher levels of genes involved in lipid metabolism, while neonatal AMs expressed a largely proinflammatory gene profile. Open enhancer regions identified by ATAC-seq contained motifs for nuclear receptors, MITF, and STAT in adult AMs and AP-1 and NF-κB in neonatal AMs. Intranasal LPS activated a similar innate immune response in both neonatal and adult mice, with higher basal expression of inflammatory genes in neonates. The lung microenvironment drove many of the distinguishing gene expression and open chromatin characteristics of neonatal and adult AMs. Neonatal mouse AMs retained high expression of some proinflammatory genes, suggesting the differences in neonatal AMs result from both inherent cell properties and environmental influences.

Address correspondence to: Lawrence S. (Lance) Prince, MD, PhD, Stanford University School of Medicine, Lucile Packard Children's Hospital Stanford, Center for Academic Medicine – 434B, Division of Neonatology - MC: 5660, 453 Quarry Road, Palo Alto, CA 94304, (650) 725-5228, lsprince@stanford.edu.

INTRODUCTION

A newborn's first breath of air is the most dramatic environmental change the pulmonary system encounters throughout the lifespan. In addition, the transition to extrauterine life involves a rapid transition of immunity from a program of fetal and maternal tolerance to protection against microbial pathogens (1–4). Macrophages are the major cells protecting the lung from infection (5). Arising initially from the primitive yolk sac, macrophages inhabit the fetal lung from the earliest stages of lung development (6). A second wave of fetal liver monocytes populates the lung later in gestation. These monocytes subsequently differentiate into alveolar macrophages in a process that requires GM-CSF and TGF-β and the transcription factors PPAR-γ, BACH2, STAT5, and CEBP-β (7–12). Differentiation of alveolar macrophages completes following birth, with increased expression of Siglec-F and CD11c and lower expression of CD11b. Newly formed alveolar macrophages take up residence in the alveolar space, recycle lipid-rich alveolar surfactant, and phagocytose inhaled particles (13). While neonatal and adult alveolar macrophages express similar cell surface markers, they may have distinct cellular functions in combatting disease.

During the time following birth, newborns are uniquely susceptible to lung disease and infection, suggesting developmental defects in immunity (14, 15). In preterm infants, infection and inflammation lead to the chronic lung disease bronchopulmonary dysplasia, the most common serious morbidity of prematurity (16). Lack of Siglec-1/sialoadhesin in lung macrophages at birth renders newborns susceptible to Group B streptococcus pneumonia (17). The increased risk of lung infection and disease in newborns suggests relative dysfunction of alveolar macrophages and neonatal innate immunity. While multiple studies suggest reduced innate immune responses in newborns (18–20), lung disease pathophysiology could also be due to excessive inflammation and inability to regulate an overzealous immune response. Consistent with this hypothesis, lung macrophages from patients that develop bronchopulmonary dysplasia have basal activation of inflammatory chemokines at birth and persistent inflammatory signatures during disease progression (21). Mechanistic differences in the neonatal and adult alveolar macrophage innate immune response may therefore contribute to the unique susceptibility of newborns to lung inflammation and pneumonia.

Throughout the body, macrophages within tissues adopt unique phenotypes and transcriptional profiles (22, 23). Tissue macrophage populations utilize core lineage dependent transcription factors including PU.1 (24). Diversity within distinct tissues relies upon additional enhancer regions that respond to tissue specific signals and subsequent transcriptional mechanisms (23). The unique alveolar microenvironment, containing GM-CSF and lipid rich surfactant, instructs transcriptional profiles in alveolar macrophages distinct from other myeloid populations in the lung and macrophages in other tissues (7, 9). The alveolar niche can also leverage cellular plasticity to stimulate alveolar macrophage differentiation. Following alveolar macrophage depletion in adult mice, macrophages and monocytes from multiple sources are each capable of differentiating into alveolar macrophages with self-renewing capacity (25). However, fetal liver monocytes are most responsive to GM-CSF signaling and proliferation. These data suggest fetal liver monocytes have inherent properties promoting their differentiation in to alveolar

macrophages. Developmentally, the relative differences between adult and neonatal lung microenvironments in promoting macrophage gene transcription remain unknown.

Here we have performed both RNA-seq and ATAC-seq on neonatal and adult mouse alveolar macrophages to define the unique transcriptomic and open chromatin landscape features at each developmental stage. Using an in vivo LPS challenge model, we also identified unique and conserved components of the innate immune response within neonatal and adult alveolar macrophages. We next demonstrated the critical role of the neonatal and adult alveolar microenvironment in directing the transcriptional profiles of alveolar macrophages. Collectively our findings define the unique features of neonatal lung alveolar macrophages, including the functional differences in how these cells regulate lung immunity during the neonatal transition period as compared to adults.

MATERIALS AND METHODS

Mice

The Institutional Animal Care and Use Committee from the University of California at San Diego approved all animal experiments. C57BL/6 mice were obtained from Envigo and bred in house. Both sexes were used for experiments up to 2 weeks of age. Male mice were used for time points between 2 to 10 weeks of age.

Intranasal Instillation of LPS

Mice were lightly anesthetized with isoflurane (MWI Veterinary Supply) before intranasal (i.n.) instillation of LPS (*Escherichia coli* O55:B5; Sigma-Aldrich) while spontaneously breathing. Neonatal (postnatal day 4, mean body weight 2.4 g) and adult (8 to 10 weeks of age, mean body weight 26 g) mice were challenged with 0.1 μg/g body weight of LPS diluted in 5 μl (neonate) or 50 μl (adult) sterile, endotoxin-free phosphate-buffered saline (PBS). Control mice received sterile PBS. All mice were euthanized 2 h after intranasal delivery of LPS or PBS.

Preparation of Cells

Following euthanasia, mouse lungs were perfused intracardially through the right ventricle with cold PBS. Lung tissue was minced and enzymatically digested in RPMI-1640 (Corning 10–040-CV) containing 50 U/ml DNase I (Roche 10104159001), 400 μg/ml Liberase TM (Roche 5401119001), and Flavopiridol (1 μM, Sigma Aldrich) at 37 °C for 15 min. Tissue homogenates were passed through a 100 μm cell strainer (Fisher Scientific), followed by erythrocyte lysis using ACK buffer (Life Technologies). Prior to antibody staining, the cell suspensions were filtered through a 70 μm cell strainer (Fisher Scientific). For isolation of cells by bronchoalveolar lavage, adult mouse lungs were lavaged via intratracheal catheter three times with 0.8-ml aliquots of cold PBS and cells were collected by centrifugation. To confirm macrophage identity, cells were immunostained using an antibody against CD68 (OriGene, FA-11) and imaged using a Leica SPE laser scanning confocal microscope.

Flow Cytometry and Cell Sorting

Single cell suspensions were resuspended in PBS with CD16/CD32 blocking antibody (Biolegend) and Zombie Aqua (Biolegend) for 20 min. The cells were then incubated with fluorochrome-conjugated antibodies in staining buffer (HBSS containing 2% FBS and 2mM EDTA) for 1h. For intracellular staining, cells were fixed and permeabilized using a Foxp3 staining buffer set as described in the manufacturer's protocol (eBiosciences). The following antibodies were used for cell sorting and analysis: CD45.2 (Biolegend, clone 104), F4/80 (Biolegend, clone BM8), CD64 (BD Biosciences, clone X54–5/7.1), Siglec-F (BD Biosciences, clone E50–2440), CD11b (Biolegend, clone M1/70), CD11c (Biolegend, clone N418), Ly-6G (Biolegend, clone 1A8), Ly-6C (BD Biosciences, clone AL-21), I-A/I-E (Biolegend, clone M5/114.15.2), and pro-IL1β (Thermo Fisher, clone NJTEN3). Samples were acquired and assessed on a BD FACSCanto II or BD FACSAria II (BD Biosciences) and analyzed with FlowJo software (FlowJo, LLC). Sorting was performed on a BD FACSAria II. Lung macrophage subsets were identified using the following gating strategy: Doublets were excluded using side scatter height (SSC-H) vs side scatter width (SSC-W), followed by forward scatter height (FSC-H) vs forward scatter width (FSC-W). Viable cells were selected using Zombie Aqua LIVE/DEAD stain. Immune cells were identified as $CD45^{+}$ cells and neutrophils were gated out using Ly-6G. Macrophages were defined as CD64 and F4/80 double-positive cells and further divided into Siglec-F^{+} $CD11b^{LO}$ AMs and Siglec-F^{-} $CD11b^{HI}$ IMs.

Primary Culture of Lung Macrophages

Freshly isolated lung macrophages were plated in 96-well plates at 60,000 to 100,000 cells/well. Culture media consisted of RPMI-1640 supplemented with 10% FBS, 100 U/mL penicillin/streptomycin, and 4 ng/mL recombinant murine M-CSF (R&D, 416-ML010). For experiments examining the effects of tissue culture environment on macrophage gene expression, cells were harvested between 0 h to 20 h of tissue culture. For studies investigating the effects of LPS on immune response of macrophages in culture, cells were stimulated with 250 ng/mL LPS (*Escherichia coli* O55:B5; Sigma-Aldrich) for 2 h either immediate after isolation or after 10 h and 20 h of tissue culture. Cells were washed with cold PBS, and then either lysed in 300 μl of TRIzol reagent (Thermo Fisher; see below) for RNA-Seq or in 50 μl lysis buffer (10 mM Tris-HCl pH7.5, 10mM NaCl, 3mM MgCl2, 0.1% IGEPAL CA-630; see below) for ATAC-Seq.

Quantitative Real-time PCR

Sorted lung macrophages were in lysed and homogenized in TRIzol reagent (Thermo Fisher) and total RNA was purified with Direct-zol RNA Miniprep columns (Zymo Research). cDNA was synthesized using SuperScript IV VILO master mix (Invitrogen). qPCR was performed using iQ SYBR Green supermix (Bio-Rad) on a CFX96 Touch Real-Time PCR Detection System (Bio-Rad). Gene expression levels were represented using $2^{-\Delta\Delta Ct}$ method and normalized to the reference gene *GAPDH*. The following primers were used: *GAPDH* Fw: 5'-AGT ATG ACT CCA CTC ACG GC-3' and *GAPDH* Rv: 5'-CAC CAG TAG ACT CCA CGA CA-3'; *Il1b* Fw: 5'-GAC CTG TTC TTT GAA GTT GAC GGA CC-3' and *Il1b* Rv: 5'-CAA TGA GTG ATA CTG CCT GCC TGA AG-3'; *Il6* Fw: 5'-AAA

CCG CTA TGA AGT TCC TCT CTG-3' and *Il6* Rv: 5'-ATC CTC TGT GAA GTC TCC TCT CC-3'; *Tnfa* Fw: 5'-ATG AGC ACA GAA AGC ATG ATC-3' and *Tnfa* Rv: 5'-TAC AGG CTT GTC ACT CGA ATT-3'.

RNA Sequencing

Purified total RNA was assessed for quality using an Agilent Tapestation 4200. Samples with an RNA Integrity Number (RIN) of at least 8.0 or greater were used to generate RNA sequencing libraries using the TruSeq Stranded mRNA Sample Prep Kit with TruSeq Unique Dual Indexes (Illumina, San Diego, CA). Total RNA (60 ng) from each sample was processed following manufacturer's specifications, adjusting RNA shear time to five minutes. Resulting RNA libraries were multiplexed and sequenced with 75 base pair (bp) single reads (SR75) to a depth of approximately 25 million reads per sample on an Illumina HiSeq 4000. Samples were demultiplexed using bcl2fastq v2.20 Conversion Software (Illumina, San Diego, CA).

ATAC Sequencing

Sorted AMs (25,000) were lysed in 25 μl lysis buffer (10 mM Tris-HCl pH7.5, 10mM NaCl, 3mM MgCl2, 0.1% IGEPAL CA-630), followed by addition of 1.25 μl Tagment DNA enzyme I (Illumina 15027865) and incubation at 37°C for 30 min. DNA was extracted with the Zymogen ChIP DNA purification kit (Zymo) and then amplified using the Nextera Primer Ad1, Nextera Barcode Primers Ad2.n, SYBR Green, and NEBNext High-Fidelity 2X PCR Master Mix for 5–15 cycles. PCR reactions were size selected for 160–280 bp by gel extraction (10% TBE gels, Life Technologies EC62752BOX) and then 75 bp single-end sequenced for 51 cycles on a HiSeq 4000.

RNA Sequencing Analysis

Quality control of the raw fastq files was performed using the software tool FastQC (26) v0.11.3. Sequencing reads were trimmed with Trimmomatic (27) v0.36 and aligned to the mouse genome (GRCm38.p6 (71) using the STAR aligner (28) v2.5.3a. Read quantification was performed with RSEM (29) v1.3.0 and the Gencode release vM19 annotation (30). The R BioConductor packages edgeR7 and limma8 were used to implement the limma-voom9 method for differential expression analysis (31–33). In brief, genes with low expression - those not having counts per million (cpm) ≥ 3 in at least 3 of the samples - were filtered out and then trimmed mean of M-values (TMM) (34) normalization was applied. The experimental design was modeled upon condition (~0 + condition). The voom method was employed to model the mean-variance relationship in the log-cpm values, after which lmFit was used to fit per-gene linear models and empirical Bayes moderation was applied with the eBayes function. Significance was defined by using an adjusted p-value cut-off of 0.05 after multiple testing correction (35) using a moderated t-statistic in limma. Functional enrichment of the differentially expressed genes was performed using IPA software (Qiagen).

ATAC Sequencing Analysis

ATAC samples were mapped to the mm10 genome using Bowtie2 (36). IDR (37) peak files were generated for each condition. Pair-wised comparisons using DESeq2 (38) were performed for all groups and specific peak subsets ($Log_2FC > 1$, p-adj < 0.05) were selected for further analysis. For the de-differentiation experiments, only peaks that were close to downregulated genes were selected. Motif analysis was performed using a specific or random background using HOMER (39) on peaks displaying significant differences. ATAC-seq data were visualized using the UCSC genome browser (40).

RESULTS

Unique transcriptional signatures differentiate adult and neonatal AMs

To identify the molecular differences between adult and newborn AMs, we compared gene expression profiles of isolated AMs from C57BL/6 mice at postnatal day 4 (P4) and 8–10 wk of age. As AMs mediate the initial immune response to microbial challenge in the lung, both adult and neonatal mice were challenged with intranasal LPS to measure potential developmental differences. Control mice received sterile, endotoxin free PBS. After 2 h, we isolated Siglec-F^+ $CD11b^{lo}$ AMs by fluorescence-activated cell sorting (FACS) (Figure 1A, Supplemental Figure S1A). Importantly, P4 represents the first day during mouse development that cell surface markers clearly identify AMs in the newborn lung. RNA-seq was performed to identify transcriptional differences between newborn and adult cells. Principal component analysis (PCA) showed that replicate samples from neonatal and adult AMs grouped together based on their transcriptional profiles (Supplemental Figure S1B).

We first compared the transcriptional profiles from PBS treated control mice to identify differences between adult and neonatal AMs at baseline. RNA-seq analysis revealed neonatal AMs contained a higher number of differentially expressed genes (1481) compared to adults (651) (fold change [Log_2FC] > 1, adjusted p [p-adj] < 0.05) (Figure 1B). Expression of AM signature genes (41) was largely similar between adult and neonatal AMs (63 of 107 signature genes with similar expression) (Figure 1C). Comparison of the representative AM genes *Cebpb, Car4,* and *Atf5* is shown in Figure 1D. The slightly higher expression of some AM signature transcripts in adult cells compared to neonates likely could represent ongoing AM maturation at P4. Neonatal AMs expressed higher levels of classical monocyte signature genes, consistent with their differentiation from fetal monocyte precursors (Figure 1D). Therefore, while the neonatal lung at P4 is populated by cells expressing adult surface markers and acquiring the AM transcriptional program, differentiation into mature AMs appeared incomplete.

We next used Ingenuity Pathway Analysis (IPA) to interrogate the functional categories of differentially expressed genes in adult and neonatal AMs (Figure 1E). Adult AMs expressed higher levels of genes related to LXR/RXR activation and PPAR signaling while neonatal AMs were enriched for genes involved in cytoskeletal dynamics, NF-κB activation, and Toll-like Receptor signaling. In illustrating these differences, adult AMs expressed higher levels of *Pparg, Fabp1, Pnpla5, Rxra,* and *Abcg1*compared to neonatal AMs, which alternatively expressed elevated levels of *Il1b*, *Tnf*, *S100a8*, *Icam1* and *Mmp12* (Figure 1F).

These data demonstrated a pro-inflammatory phenotype in neonatal AMs when compared to adult cells. AMs derive from fetal liver monocytes that are more pro-inflammatory when compared to yolk sac derived macrophages (42). However, the influences of parturition, delivery, and postnatal AM differentiation on this inflammatory program are unknown. To better understand the dynamics of this phenotype, we measured *Il1b* expression in FACS sorted lung macrophages during fetal development, at birth, and into adulthood (Figure 1G). *Il1b* expression increased in AM precursors during late gestation, peaked on the day of delivery, and fell in differentiated, more mature AMs. The fetal lung therefore appeared to further promote the inflammatory program of AM precursors. The peak expression at birth could also reflect inflammatory activation as part of the timing of parturition. Collectively, these data demonstrate that differentiating neonatal AMs possess a very distinct transcriptional profile related to activation of the innate immune response.

Distinct transcriptional regulators inferred from open chromatin profiles

To gain insights into potential epigenetic mechanisms underlying the differential transcriptional programs of adult and neonatal AMs, we identified open chromatin regions using an assay for transposase-accessible chromatin sequencing (ATAC-seq). ATAC-seq allowed us to identify regions of accessible chromatin at a single nucleotide level, exposing potential enhancer regions available to transcription factors. The ATAC-seq tracks illustrated in Figure 2A highlight examples of chromatin regions that are similarly and differentially accessible. We found genes critical for macrophage and AM lineage determination and differentiation, such as *Spi1* and *Pparg*, exhibited similar open chromatin profiles at putative regulatory elements in neonatal and adult AMs. In contrast, chromatin regions adjacent to *Chil3* and *Fabp1* were more accessible in adult AMs. Upregulation of macrophage marker *Chil3* (encoding Ym1) has been previously described with AM differentiation and alternatively activated macrophage populations (43, 44). Neonatal AMs contained more open chromatin regions neighboring the platelet-derived growth factor member *Pdgfa* and the monocyte marker *Ly6c2*. *Pdgfa* is expressed in both lung macrophages and epithelial cells and plays a key role in postnatal alveolar septation (45, 46). The *Ly6c2* signal could be consistent with incomplete chromatin remodeling and gene silencing during differentiation of monocyte-derived neonatal AMs.

Genome-wide comparison of ATAC-seq peak tag counts identified 1852 genomic sites with differentially open chromatin between adult (835) and neonatal (1017) AMs (Figure 2B). The open chromatin enhancer regions (>2 kb from a transcription start site (TSS)) in adult AMs contained motifs predicted to bind MITF, STAT5, and a halfsite for nuclear receptors (NR; Figure 2C). Neonatal-enriched regions exhibited significant overrepresentation of motifs for AP-1, NF-κB, and the nuclear receptor Nur77. These enrichments are consistent with adult AMs being exposed to prolonged GM-CSF (STAT5) and nuclear receptor agonists. The presence of AP-1 and NF-κB sites in neonatal AMs aligns with the proinflammatory transcriptional profile measured by RNAseq (Figure 1, Supplemental Figure S1D).

We next compared the expression levels of TF family members whose motifs were predicted by ATAC-seq, focusing primarily on TF with expression above 16 CPM and with differential

expression between adult and neonatal AMs (Figure 2D,E). All three MITF family members were more prevalent in adult AMs. While *Stat1*, *Stat3*, and *Stat6* were most abundant overall, *Stat2*, *Stat5a*, and *Stat5b* were more differentially expressed in adult AMs compared to neonatal cells. Adult AMs expressed high levels of the nuclear receptors *Pparg, Rora, Rxra,* and the glucocorticoid receptor *Nr3c1,* each with specific roles in AM maturation and inflammatory responses (9, 47–49). Neonatal AMs expressed higher levels of multiple AP-1 family members compared to adult AMs (Figure 2E), with highest expression of the AP-1 family members *Junb*, *Fosl2*, and *Atf4*. NF-κB family members *Nfkb1*, *Nfkb2*, *Relb*, and *Rel* were all more highly expressed in neonatal AMs (Figure 2E). Interestingly, expression of the nuclear receptor *Nr4a1*, encoding Nur77, was higher in neonatal AM but with overall low expression throughout. Together, these data link the differential transcription signatures in neonatal and adult AM with TF expression and enhancer availability.

Innate immune response of neonatal and adult AMs

Data from control AMs clearly demonstrated a more pro-inflammatory phenotype in neonatal AMs. However, this pattern of gene transcription represented baseline conditions and did not address macrophage function following microbial challenge. We therefore compared the response of adult and neonatal AMs following brief (2 h) intranasal LPS challenge to test for potential differences in the early innate immune response. LPS induced robust recruitment of neutrophils and monocytes into adult lungs, consistent with acute lung inflammatory response (Figure S2A,B). The recruitment of additional $CD45^+$ cells into the lung, along with potential programmed cell death, likely contributed to the reduction in the relative percentage of AMs. In neonatal lungs, LPS stimulated similar changes but with more moderate neutrophil increases and AM reduction. Both AMs and Siglec-F^- lung interstitial macrophages and monocytes (IM/Mo) are known to respond to inflammatory stimuli (50, 51). To confirm the cellular sites of stimulation following in vivo LPS treatment, we measured pro-IL-1β expression in both macrophage populations (Figure S2C,D). Consistent with RNAseq data (Figure 1G,F), AMs from neonates expressed baseline levels of pro-IL-1β. The percentage of pro-IL-1β-positive AMs following LPS exposure was similar in neonates and adults. A smaller percentage of IM also expressed IL-1β after LPS exposure, with again similar response between adults and neonates (Figure S2D). These results identified AMs as the major cellular site of innate immune activation in both adult and neonatal lungs in response to inhaled LPS, consistent with their location in the alveolar space. Importantly, these data did not identify significant differences in LPS-dependent IL-1β expression between neonates and adults.

RNA-seq analysis of isolated AMs following LPS exposure identified more differentially expressed genes in adults (2207) compared to neonates (950) ($Log_2FC > 2$, p-adj < 0.05) (Figure 3A). IPA functional analysis of differentially expressed genes following in vivo LPS treatment included the major pathways downstream of the LPS receptor TLR4 (Toll-like receptor signaling, NF-κB signaling, and p38 MAPK signaling, Figure 3B). One notable difference was the upregulation of genes associated with interferon signaling in adult AMs.

At first glance, the increased number of LPS-activated transcripts in adult AMs might suggest a more robust innate immune response in adults compared to neonates. However,

control neonatal AMs expressed higher levels of transcripts involved in inflammation and TLR4 signaling pathways (Figure 3C). Consistently, a majority of LPS-activated genes ($Log_2FC > 2$, p-adj < 0.05) were expressed at higher levels in neonatal cells under control, baseline conditions (genes above the diagonal in Figure 3C). These data suggested the higher baseline expression of LPS-activated genes in neonates accounted for the reduced fold-change in many genes after LPS exposure. Of the 1119 upregulated genes in adults and 669 upregulated genes in neonates, 480 were shared (Figure 3D). When we examined the expression of LPS-activated transcripts in control samples, we observed that most had either similar expression under control conditions or higher expression in control neonates and were only rarely expressed higher in adult cells (Figure 3E). Specific examples of genes are highlighted in Figure 3F. LPS induced high levels of inflammatory mediators in both neonatal and adult cells, exemplified by *Il1b*, *Ccl3, Il6*, *and Tnf*. While these genes exhibited similar expression level after LPS, elevated basal expression in neonatal cells resulted in a lower LPS-activated fold change compared to adult cells. Among the genes activated in adult AMs, the expression levels of *Ikbke*, *S100a8*, and *Irf5* were examples of genes also more highly expressed in neonatal AMs at baseline. Higher control expression was also measured for many genes primarily upregulated in neonatal cells. Collectively, these data demonstrate that neonatal AMs can mount a robust innate immune response to LPS in vivo, with the most notable differences compared to adults being due to higher expression of inflammatory genes under control, baseline conditions.

Intranasal LPS rapidly reprograms the AM chromatin landscape in vivo

We next tested how in vivo innate immune activation with LPS changes the regulatory landscape of adult and neonatal AMs. Figure 4A illustrates examples of ATAC-seq peaks that exhibited overlapping changes in the open chromatin pattern after LPS exposure. Strongly induced pro-inflammatory genes, including *Il1b*, *Ccl4*, and *Nfkbia*, exhibited an increase in ATAC-seq peak number and amplitude, consistent with LPS-induced changes in chromatin structure. Genome-wide comparison of open chromatin regions between LPS treated and control AMs identified genomic sites with differentially accessible chromatin in adults and neonates (Figure 4B).

Known motif analysis of ATAC-seq peaks following LPS activation identified conserved innate immunity transcription factor binding motifs (Figure 4C). Both adult and neonatal sequences contained motifs assigned to STAT, NF-κB, and AP-1 family members, with similar relative abundance of these motifs in open chromatin regions following LPS stimulation. To infer the likely TFs responsible for induction of inflammatory response in each AMs, we compared gene expression of family members recognizing the enriched motifs (Figure 4D). STAT family members were more highly expressed in adults and increased following LPS exposure. Expression of AP-1 family members were increased by LPS, with some subunits differentially expressed in adult and neonatal cells. Members of the NF-κB family *(Nfkb1, Nfkb2, Rela, Relb, and Rel)* were all increased after LPS and expressed at comparable levels between adult and neonatal cells. Collectively, these results show that adult and neonatal AMs use canonical regulatory mechanisms in mediating the in vivo innate immune response upon TLR activation. However, differences in STAT signaling,

expression of specific AP-1 family members, or availability of open chromatin throughout the genome could account for differences in the transcriptional response.

The lung microenvironment drives unique transcriptional signatures in adult and neonatal AMs

Tissue specific microenvironments instruct unique macrophage phenotypes in different organs, but the impact of development and age on tissue effects are unclear. We tested whether the differences in neonatal and adult AM gene expression, in particular the pro-inflammatory signature measured in neonatal AMs, was due to inherent developmental programs or differences in the adult and neonatal lung microenvironments. We first measured expression of several known AM signature genes in adult AMs following isolation and culture. Interestingly, expression of the pan-macrophage marker *Spi1* (encoding PU.1) remained consistent over time, while expression of more AM-specific genes (*Pparg* and *Car4*) rapidly decreased following removal from the lung (Supplemental Figure S3B). We next used RNA-seq to measure how the adult and neonatal lung microenvironment might direct global AM transcriptional programs. PCA analysis illustrated how 20 h of culture altered overall transcription in both neonatal and adult cells (Figure 5A). The transition into culture reduced expression of many AM genes (below the diagonal in Figure 5B). In addition, the divergent transcriptional profiles between adult and neonatal AMs converged following removal from the lung microenvironment (Figure 5C). The heat-map visualization in Figure 5D highlights genes enriched in adult or neonatal cells that were highly sensitive to environmental change. The expression of nearly half of the adult-enriched genes was altered in culture (Figure 5E), whereas changing the microenvironment only altered about 10% of genes shared in common between adult and neonatal AMs. Similar effects were measured in genes enriched in neonatal AMs. These results suggested that the adult and neonatal lung microenvironments are required for many of the unique transcriptional differences between the different developmental stages. However, inflammatory genes enriched in neonatal AMs were not consistently impacted by culture (Figure 5F), suggesting that at least a component of the proinflammatory signature in neonatal AM was inherent and not environmentally sensitive.

Environmental impact on AM chromatin landscapes

To investigate how the lung microenvironment might regulate AM-specific transcription, we next examined AM TF expression from our RNA-seq dataset. Expression of the pan-macrophage factor *Spi1* was maintained in culture, albeit slightly reduced in cultured neonatal AMs (Figure 6A). However, culturing AMs reduced expression of the AM-specific TFs *Pparg*, *Cebpb*, and *Atf5*. We next tested the impact of the in vivo lung microenvironment in regulating innate immune function. Adult and neonatal AMs were stimulated with LPS either immediately after isolation or after placement in tissue culture. For both adults and neonates, longer culture times enhanced LPS-stimulated cytokine expression (Figure 6B). As basal cytokine expression did not increase in culture, these results suggest that both adult and neonatal lung microenvironments actively work to temper innate immune inflammatory responses.

The lung microenvironment also regulated expression of the key TFs identified in Figure 2. In adult cells, in vitro culture reduced expression of the MITF family member *Tfec* and multiple nuclear receptors (Figure 6C). Removal of neonatal AMs from the lung microenvironment decreased expression of multiple AP-1 family members and *Nr4a1*, while slightly increasing NF-κB family members. Therefore, the lung microenvironment was required for expression of key TFs regulating AM function and components of the innate immune response. Next, we performed ATAC-seq to measure the impact of removing AMs from the lung microenvironment on the epigenetic landscape. In both adult and neonatal cells, de novo motif analysis identified loss of sequences recognized by PU.1, CEBP, and KLF following removal from the lung (Figure 6D). In addition to these common motifs, the analysis also recovered motifs specific for neonates and adults. For example, ATAC-seq peaks associated with downregulated genes in adult AMs were enriched for MITF and ATF motifs. In neonatal AMs, NFIL3 and AP-1 motifs were associated with reduced gene expression in culture. Figure 6E illustrates examples of ATAC-seq peaks that exhibit substantial reduction in the vicinity of downregulated genes after culturing. These data emphasize the critical role of the tissue environment in establishing gene regulatory landscapes unique to adult and neonatal AMs.

DISCUSSION

Here we have identified the molecular features differentiating AMs within adult and neonatal mouse lungs. While both neonatal and adult AMs express common surface markers and AM signature genes, differences in expression may provide the basis for developmental differences in lung immunity. Neonatal AMs expressed a distinct proinflammatory transcriptional signature. In contrast, adult AMs were enriched for genes associated with fatty acid metabolism and lipid-mediated signaling. Despite the molecular differences under basal conditions, both neonatal and adult AMs elicited robust in vivo responses to inhaled LPS. These data demonstrate both core functional properties and unique expression patterns within AMs at different stages of development.

The inflammatory transcripts in neonatal AMs were enriched with enhancer sequences predicted to bind the canonical innate immune TFs AP-1 and NF-κB. Many of the genes expressed at higher levels in neonatal AMs under basal conditions were subsequently increased by in vivo LPS exposure. These data suggested a pre-activated or primed inflammatory state in neonatal AMs. Similarly, fetal liver-derived macrophages, which give rise to alveolar macrophages, exhibit a pro-inflammatory phenotype within various tissues when compared to yolk sac-derived macrophages (42). As a marker for this pro-inflammatory signature, *Il1b* expression in lung macrophages increased during late gestation, peaked at birth, and decreased following birth into adulthood. The inflammatory profile of macrophages around birth could be related to the normal physiologic connection between inflammation and the onset of parturition (52, 53). While the timing of gestation is multifactorial, lung maturation may play a role in stimulating innate immune pathways and the onset of labor (54–56). The normal physiology of parturition could therefore impart the pro-inflammatory signature upon neonatal AMs.

During pregnancy, fetal and maternal immune systems maintain a tolerant state (57, 58). Possibly as a consequence, human newborns are particularly susceptible to lung infections acquired at delivery (59). Within the neonatal lung, primed AMs with basal innate immune activation might provide protection against microbes. However, this activated phenotype in neonatal AMs could lead to exaggerated and uncontrolled inflammation, especially in infants born preterm. The inflammatory expression pattern in neonatal AMs might also be augmented by the sudden exposure to the extrauterine environment (60). In human preterm infants, inflammatory gene expression in AM in some patients at birth correlated with development of more severe chronic lung disease (21). Whether these early disease risk patterns are due to inherent cell programming at birth or external factors remains to be investigated.

Lipid-rich surfactant and the alveolar microenvironment could instruct differentiated AMs to steadily acquire a more tolerant, quiescent baseline phenotype via nuclear receptor signaling. Importantly, this observed “tolerance” profile did not compromise the adult AM response to LPS. In the lung, IL-10 and TGF-β likely each promote a more tolerant, mature phenotype in adult AMs (8, 61). The cell surface receptors Axl and Mertk suppress inflammatory macrophage activation (62), however their expression was similar in adult and neonatal AMs (data not shown). Adult AMs expressed higher levels of *Pparg*, *Stat5*, and *Nr3c1*, each implicated in AM maturation and inflammatory regulation (9, 11, 63, 64). GM-CSF, TGF-β, and lipid agonists can increase *Pparg* expression or directly lead to its activation in developing AMs and other macrophage populations (8, 9, 65). Indispensable for AM differentiation, PPAR-γ can also function as an E3 ligase and target the p65 subunit of NF-κB for proteasomal degradation (66). Activation of the glucocorticoid receptor encoded by *Nr3c1* inhibits NF-κB mediated inflammation via multiple transcriptional mechanisms (67, 68). Neonatal AM expressed genes with enriched availability of the nuclear receptor NR4A1 (Nur77), which negatively influences macrophage inflammation and lung injury (69, 70). However, *Nr4a1* expression in both neonatal and adult AMs is relatively low, and its relative influence compared to other nuclear receptors in the newborn lung is not yet known.

Both adult and neonatal AMs mounted a robust innate immune response in vivo when challenged with intranasal LPS. Transcriptional changes and chromatin dynamics (as measured by RNA-seq and ATAC-seq) demonstrated a canonical response employing the signal-dependent transcription factors AP-1 and NF-κB. A major difference between neonates and adults following LPS exposure was the smaller number of DE genes in neonatal AMs compared to LPS-treated adult AMs. Reduced stimulation of pro-inflammatory cytokines, such as *Il1b*, *Il6*, and *Tnf* in neonatal cells, might suggest an immunocompromised or tolerant state in newborns (15, 71–73). However, we found the absolute gene expression levels after LPS treatment were comparable between adult and neonatal AMs, with the elevated basal expression levels in neonatal cells leading to a reduced LPS-activated fold change. We therefore suggest a more global context is necessary in determining whether or not the innate immune response of newborns is truly deficient when compared to adults.

The lung microenvironment was required for the unique transcriptional profiles of neonatal and adult AMs. Transferring isolated AMs to a cell culture environment led to profound and rapid changes in gene expression. While the expression of the pan-macrophage marker *Spi1* and a majority of genes shared between neonatal and adult AMs held constant, cell culture quickly reduced expression of AM signature genes and many of the genes differentially expressed between adult and neonatal AMs. The lung microenvironment therefore contains signals required for establishing AM identity at each developmental age. Similar requirements of the tissue microenvironment were observed with microglia (74). Intriguingly, the inflammatory phenotype of neonatal AMs was partially conserved in culture. While cell culture reduced expression of many AP-1 subunits in neonatal AMs, expression of NF-κB family members persisted. The pro-inflammatory, innate immune program in neonatal AMs is therefore likely instructed by both cell-autonomous and environmentally regulated mechanisms. Unique, specialized cell culture conditions may be able to preserve the specific aspects of alveolar macrophage gene expression. These data do emphasize the importance of investigating macrophage biology using in vivo models and considering the tissue microenvironment.

Our findings add another layer to the current knowledge regarding the developmental program of AM identity and function. Proinflammatory AM precursors migrate from the liver to the lung in the developing fetus (42). Once in the lung, the inflammatory signature increases leading up to birth and persists as these macrophages differentiate into mature AM in the days following delivery. Additional factors such as developmental regulation of cell surface receptors may further regulate tolerance or immune activation in these differentiating macrophage populations (17). We propose changes in the lung environment around the time of birth promote expression of inflammatory genes in AM precursors. The dramatic environmental changes at birth, including clearance of amniotic fluid, initiation of breathing and exposure to oxygen, and inhalation of commensal and pathogenic microbes, could each drive inflammatory gene expression. However, our data here show that *Il1b* expression increased in fetal lung monocytes prior to delivery. The inflammatory phenotype of AMs under basal conditions was then steadily dampened during postnatal development into adulthood. Maturation of AMs correlates with acquisition of alternatively activated (or M2) macrophage markers (75). In spite of this phenotype, mature adult AMs clearly responded to the classic M1 agonist LPS. The M1/M2 paradigm described in tumor associated macrophages and chronic inflammatory models may therefore not apply as clearly to the alveolar environment. Further identification of the molecular mechanisms regulating adult and neonatal immune states could further our understanding of lung injury, repair, and regeneration in a variety of disease states.

Supplementary Material

Refer to Web version on PubMed Central for supplementary material.

ACKNOWLEDGEMENTS

The authors thank Hal Hoffman, Lori Broderick, Victor Nizet, Alyssa McCoy, Gilberto Hernandez, Tomoya Honda, and members of the Prince and Glass laboratories for their helpful advice and guidance throughout this project.

This work was supported by the National Institutes of Health grants HL126703 (L. S. Prince), HL143256 (L. S. Prince and E. Sajti), HL146066 (S. J. Lund), HL148867 (E. Sajti), HL140198 (E. Sajti), HL147835 (C. K. Glass and M. Sakai), and an American Heart Association Fellowship (M. A. Hoeksema). This work was performed with the support of the Flow Cytometry Core at the San Diego Center for AIDS Research (P30 AI036214), the VA San Diego Health Care System, and the San Diego Veterans Medical Research Foundation. The project was partially supported by the National Institutes of Health grant UL1TR001442 of the University of California, San Diego Clinical and Translational Science Award Program.

REFERENCES

1. Kostlin-Gille N, and Gille C. 2020. Myeloid-Derived Suppressor Cells in Pregnancy and the Neonatal Period. Front Immunol 11: 584712.
2. Guleria I, and Sayegh MH 2007. Maternal acceptance of the fetus: true human tolerance. J Immunol 178: 3345–3351. [PubMed: 17339426]
3. Mold JE, Michaelsson J, Burt TD, Muench MO, Beckerman KP, Busch MP, Lee TH, Nixon DF, and McCune JM 2008. Maternal alloantigens promote the development of tolerogenic fetal regulatory T cells in utero. Science 322: 1562–1565. [PubMed: 19056990]
4. Kollmann TR, Marchant A, and Way SS 2020. Vaccination strategies to enhance immunity in neonates. Science 368: 612–615. [PubMed: 32381718]
5. Garbi N, and Lambrecht BN 2017. Location, function, and ontogeny of pulmonary macrophages during the steady state. Pflugers Arch 469: 561–572. [PubMed: 28289977]
6. Perdiguero EG, and Geissmann F. 2016. The development and maintenance of resident macrophages. Nat Immunol 17: 2–8. [PubMed: 26681456]
7. Guilliams M, De Kleer I, Henri S, Post S, Vanhoutte L, De Prijck S, Deswarte K, Malissen B, Hammad H, and Lambrecht BN 2013. Alveolar macrophages develop from fetal monocytes that differentiate into long-lived cells in the first week of life via GM-CSF. J Exp Med 210: 1977–1992. [PubMed: 24043763]
8. Yu X, Buttgereit A, Lelios I, Utz SG, Cansever D, Becher B, and Greter M. 2017. The Cytokine TGF-beta Promotes the Development and Homeostasis of Alveolar Macrophages. Immunity 47: 903–912 e904. [PubMed: 29126797]
9. Schneider C, Nobs SP, Kurrer M, Rehrauer H, Thiele C, and Kopf M. 2014. Induction of the nuclear receptor PPAR-gamma by the cytokine GM-CSF is critical for the differentiation of fetal monocytes into alveolar macrophages. Nat Immunol 15: 1026–1037. [PubMed: 25263125]
10. Nakamura A, Ebina-Shibuya R, Itoh-Nakadai A, Muto A, Shima H, Saigusa D, Aoki J, Ebina M, Nukiwa T, and Igarashi K. 2013. Transcription repressor Bach2 is required for pulmonary surfactant homeostasis and alveolar macrophage function. J Exp Med 210: 2191–2204. [PubMed: 24127487]
11. Eddy WE, Gong KQ, Bell B, Parks WC, Ziegler SF, and Manicone AM 2017. Stat5 Is Required for CD103(+) Dendritic Cell and Alveolar Macrophage Development and Protection from Lung Injury. J Immunol 198: 4813–4822. [PubMed: 28500076]
12. Cain DW, O'Koren EG, Kan MJ, Womble M, Sempowski GD, Hopper K, Gunn MD, and Kelsoe G. 2013. Identification of a tissue-specific, C/EBPbeta-dependent pathway of differentiation for murine peritoneal macrophages. J Immunol 191: 4665–4675. [PubMed: 24078688]
13. Ueda T, Ikegami M, Henry M, and Jobe AH 1995. Clearance of surfactant protein B from rabbit lungs. Am J Physiol 268: L636–641. [PubMed: 7733304]
14. Liu L, Johnson HL, Cousens S, Perin J, Scott S, Lawn JE, Rudan I, Campbell H, Cibulskis R, Li M, Mathers C, Black RE, Child WHO Health Epidemiology Reference Group of, and Unicef. 2012. Global, regional, and national causes of child mortality: an updated systematic analysis for 2010 with time trends since 2000. Lancet 379: 2151–2161. [PubMed: 22579125]
15. Dowling DJ, and Levy O. 2014. Ontogeny of early life immunity. Trends Immunol 35: 299–310. [PubMed: 24880460]
16. Sucre J, Haist L, Bolton CE, and Hilgendorff A. 2021. Early Changes and Indicators Characterizing Lung Aging in Neonatal Chronic Lung Disease. Front Med (Lausanne) 8: 665152.
17. Lund SJ, Patras KA, Kimmey JM, Yamamura A, Butcher LD, Del Rosario PGB, Hernandez GE, McCoy AM, Lakhdari O, Nizet V, and Prince LS 2020. Developmental Immaturity of

Siglec Receptor Expression on Neonatal Alveolar Macrophages Predisposes to Severe Group B Streptococcal Infection. iScience 23: 101207.

18. La Pine TR, Joyner JL, Augustine NH, Kwak SD, and Hill HR 2003. Defective production of IL-18 and IL-12 by cord blood mononuclear cells influences the T helper-1 interferon gamma response to group B Streptococci. Pediatr Res 54: 276–281. [PubMed: 12736393]
19. Lee SM, Suen Y, Chang L, Bruner V, Qian J, Indes J, Knoppel E, van de Ven C, and Cairo MS 1996. Decreased interleukin-12 (IL-12) from activated cord versus adult peripheral blood mononuclear cells and upregulation of interferon-gamma, natural killer, and lymphokine-activated killer activity by IL-12 in cord blood mononuclear cells. Blood 88: 945–954. [PubMed: 8704253]
20. Kollmann TR, Crabtree J, Rein-Weston A, Blimkie D, Thommai F, Wang XY, Lavoie PM, Furlong J, Fortuno ES 3rd, Hajjar AM, Hawkins NR, Self SG, and Wilson CB 2009. Neonatal innate TLR-mediated responses are distinct from those of adults. J Immunol 183: 7150–7160. [PubMed: 19917677]
21. Sahoo D, Zaramela LS, Hernandez GE, Mai U, Taheri S, Dang D, Stouch AN, Medal RM, McCoy AM, Aschner JL, Blackwell TS, Zengler K, and Prince LS 2020. Transcriptional profiling of lung macrophages identifies a predictive signature for inflammatory lung disease in preterm infants. Commun Biol 3: 259. [PubMed: 32444859]
22. Mass E, Ballesteros I, Farlik M, Halbritter F, Gunther P, Crozet L, Jacome-Galarza CE, Handler K, Klughammer J, Kobayashi Y, Gomez-Perdiguero E, Schultze JL, Beyer M, Bock C, and Geissmann F. 2016. Specification of tissue-resident macrophages during organogenesis. Science 353.
23. Lavin Y, Winter D, Blecher-Gonen R, David E, Keren-Shaul H, Merad M, Jung S, and Amit I. 2014. Tissue-resident macrophage enhancer landscapes are shaped by the local microenvironment. Cell 159: 1312–1326. [PubMed: 25480296]
24. Gosselin D, Link VM, Romanoski CE, Fonseca GJ, Eichenfield DZ, Spann NJ, Stender JD, Chun HB, Garner H, Geissmann F, and Glass CK 2014. Environment drives selection and function of enhancers controlling tissue-specific macrophage identities. Cell 159: 1327–1340. [PubMed: 25480297]
25. van de Laar L, Saelens W, De Prijck S, Martens L, Scott CL, Van Isterdael G, Hoffmann E, Beyaert R, Saeys Y, Lambrecht BN, and Guilliams M. 2016. Yolk Sac Macrophages, Fetal Liver, and Adult Monocytes Can Colonize an Empty Niche and Develop into Functional Tissue-Resident Macrophages. Immunity 44: 755–768. [PubMed: 26992565]
26. Andrews S. 2010. FastQC: a quality control tool for high throughput sequence data. Babraham Bioinformatics, Babraham Institute, Cambridge, United Kingdom.
27. Bolger AM, Lohse M, and Usadel B. 2014. Trimmomatic: a flexible trimmer for Illumina sequence data. Bioinformatics 30: 2114–2120. [PubMed: 24695404]
28. Dobin A, Davis CA, Schlesinger F, Drenkow J, Zaleski C, Jha S, Batut P, Chaisson M, and Gingeras TR 2013. STAR: ultrafast universal RNA-seq aligner. Bioinformatics 29: 15–21. [PubMed: 23104886]
29. Li B, and Dewey CN 2011. RSEM: accurate transcript quantification from RNA-Seq data with or without a reference genome. BMC bioinformatics 12: 323. [PubMed: 21816040]
30. Frankish A, Diekhans M, Ferreira A-M, Johnson R, Jungreis I, Loveland J, Mudge JM, Sisu C, Wright J, and Armstrong J. 2019. GENCODE reference annotation for the human and mouse genomes. Nucleic acids research 47: D766–D773. [PubMed: 30357393]
31. Robinson MD, McCarthy DJ, and Smyth GK 2010. edgeR: a Bioconductor package for differential expression analysis of digital gene expression data. Bioinformatics 26: 139–140. [PubMed: 19910308]
32. Ritchie ME, Phipson B, Wu D, Hu Y, Law CW, Shi W, and Smyth GK 2015. limma powers differential expression analyses for RNA-sequencing and microarray studies. Nucleic Acids Res 43: e47. [PubMed: 25605792]
33. Law CW, Chen Y, Shi W, and Smyth GK 2014. voom: Precision weights unlock linear model analysis tools for RNA-seq read counts. Genome Biol 15: R29. [PubMed: 24485249]
34. Robinson MD, and Oshlack A. 2010. A scaling normalization method for differential expression analysis of RNA-seq data. Genome biology 11: 1–9.

35. Benjamini Y, and Hochberg Y. 1995. Controlling the false discovery rate: a practical and powerful approach to multiple testing. Journal of the Royal statistical society: series B (Methodological) 57: 289–300.
36. Langmead B, and Salzberg SL 2012. Fast gapped-read alignment with Bowtie 2. Nature methods 9: 357. [PubMed: 22388286]
37. Li Q, Brown JB, Huang H, and Bickel PJ 2011. Measuring reproducibility of high-throughput experiments. The annals of applied statistics 5: 1752–1779.
38. Love MI, Huber W, and Anders S. 2014. Moderated estimation of fold change and dispersion for RNA-seq data with DESeq2. Genome biology 15: 550. [PubMed: 25516281]
39. Heinz S, Benner C, Spann N, Bertolino E, Lin YC, Laslo P, Cheng JX, Murre C, Singh H, and Glass CK 2010. Simple combinations of lineage-determining transcription factors prime cis-regulatory elements required for macrophage and B cell identities. Mol Cell 38: 576–589. [PubMed: 20513432]
40. Kent WJ, Sugnet CW, Furey TS, Roskin KM, Pringle TH, Zahler AM, and Haussler D. 2002. The human genome browser at UCSC. Genome research 12: 996–1006. [PubMed: 12045153]
41. Gautier EL, Shay T, Miller J, Greter M, Jakubzick C, Ivanov S, Helft J, Chow A, Elpek KG, Gordonov S, Mazloom AR, Ma'ayan A, Chua WJ, Hansen TH, Turley SJ, Merad M, Randolph GJ, and Immunological Genome C. 2012. Gene-expression profiles and transcriptional regulatory pathways that underlie the identity and diversity of mouse tissue macrophages. Nat Immunol 13: 1118–1128. [PubMed: 23023392]
42. Lakhdari O, Yamamura A, Hernandez GE, Anderson KK, Lund SJ, Oppong-Nonterah GO, Hoffman HM, and Prince LS 2019. Differential Immune Activation in Fetal Macrophage Populations. Sci Rep 9: 7677. [PubMed: 31118442]
43. Gordon S. 2003. Alternative activation of macrophages. Nature reviews immunology 3: 23–35.
44. Stouch AN, Zaynagetdinov R, Barham WJ, Stinnett AM, Slaughter JC, Yull FE, Hoffman HM, Blackwell TS, and Prince LS 2014. IkappaB kinase activity drives fetal lung macrophage maturation along a non-M1/M2 paradigm. J Immunol 193: 1184–1193. [PubMed: 24981452]
45. Gouveia L, Betsholtz C, and Andrae J. 2018. PDGF-A signaling is required for secondary alveolar septation and controls epithelial proliferation in the developing lung. Development 145.
46. Liu JY, Morris GF, Lei WH, Hart CE, Lasky JA, and Brody AR 1997. Rapid activation of PDGF-A and -B expression at sites of lung injury in asbestos-exposed rats. Am J Respir Cell Mol Biol 17: 129–140. [PubMed: 9271299]
47. Nejati Moharrami N, Bjorkoy Tande E, Ryan L, Espevik T, and Boyartchuk V. 2018. RORalpha controls inflammatory state of human macrophages. PLoS One 13: e0207374.
48. Roszer T, Menendez-Gutierrez MP, Cedenilla M, and Ricote M. 2013. Retinoid X receptors in macrophage biology. Trends Endocrinol Metab 24: 460–468. [PubMed: 23701753]
49. Cain DW, and Cidlowski JA 2017. Immune regulation by glucocorticoids. Nat Rev Immunol 17: 233–247. [PubMed: 28192415]
50. Fan J, Kapus A, Marsden PA, Li YH, Oreopoulos G, Marshall JC, Frantz S, Kelly RA, Medzhitov R, and Rotstein OD 2002. Regulation of Toll-like receptor 4 expression in the lung following hemorrhagic shock and lipopolysaccharide. J Immunol 168: 5252–5259. [PubMed: 11994482]
51. Sajti E, Link VM, Ouyang Z, Spann NJ, Westin E, Romanoski CE, Fonseca GJ, Prince LS, and Glass CK 2020. Transcriptomic and epigenetic mechanisms underlying myeloid diversity in the lung. Nat Immunol 21: 221–231. [PubMed: 31959980]
52. Hadley EE, Richardson LS, Torloni MR, and Menon R. 2018. Gestational tissue inflammatory biomarkers at term labor: A systematic review of literature. Am J Reprod Immunol 79.
53. Cappelletti M, Doll JR, Stankiewicz TE, Lawson MJ, Sauer V, Wen B, Kalinichenko VV, Sun X, Tilburgs T, and Divanovic S. 2020. Maternal regulation of inflammatory cues is required for induction of preterm birth. JCI Insight 5.
54. Madhukaran SP, Alhamlan FS, Kale K, Vatish M, Madan T, and Kishore U. 2016. Role of collectins and complement protein C1q in pregnancy and parturition. Immunobiology 221: 1273–1288. [PubMed: 27349595]

55. Montalbano AP, Hawgood S, and Mendelson CR 2013. Mice deficient in surfactant protein A (SP-A) and SP-D or in TLR2 manifest delayed parturition and decreased expression of inflammatory and contractile genes. Endocrinology 154: 483–498. [PubMed: 23183169]
56. Condon JC, Jeyasuria P, Faust JM, and Mendelson CR 2004. Surfactant protein secreted by the maturing mouse fetal lung acts as a hormone that signals the initiation of parturition. Proc Natl Acad Sci U S A 101: 4978–4983. [PubMed: 15044702]
57. Teirila L, Heikkinen-Eloranta J, Kotimaa J, Meri S, and Lokki AI 2019. Regulation of the complement system and immunological tolerance in pregnancy. Semin Immunol 45: 101337.
58. Ander SE, Diamond MS, and Coyne CB 2019. Immune responses at the maternal-fetal interface. Sci Immunol 4.
59. Campbell JR 1996. Neonatal pneumonia. Semin Respir Infect 11: 155–162. [PubMed: 8883173]
60. Choi Y, Rekers L, Dong Y, Holzfurtner L, Goetz MJ, Shahzad T, Zimmer KP, Behnke J, Behnke J, Bellusci S, and Ehrhardt H. 2021. Oxygen Toxicity to the Immature Lung-Part I: Pathomechanistic Understanding and Preclinical Perspectives. Int J Mol Sci 22.
61. Laubreton D, Drajac C, Eleouet JF, Rameix-Welti MA, Lo-Man R, Riffault S, and Descamps D. 2020. Regulatory B Lymphocytes Colonize the Respiratory Tract of Neonatal Mice and Modulate Immune Responses of Alveolar Macrophages to RSV Infection in IL-10-Dependant Manner. Viruses 12.
62. Fujimori T, Grabiec AM, Kaur M, Bell TJ, Fujino N, Cook PC, Svedberg FR, MacDonald AS, Maciewicz RA, Singh D, and Hussell T. 2015. The Axl receptor tyrosine kinase is a discriminator of macrophage function in the inflamed lung. Mucosal Immunol 8: 1021–1030. [PubMed: 25603826]
63. Nobs SP, and Kopf M. 2018. PPAR-gamma in innate and adaptive lung immunity. J Leukoc Biol 104: 737–741. [PubMed: 29768688]
64. Culpitt SV, Rogers DF, Shah P, De Matos C, Russell RE, Donnelly LE, and Barnes PJ 2003. Impaired inhibition by dexamethasone of cytokine release by alveolar macrophages from patients with chronic obstructive pulmonary disease. Am J Respir Crit Care Med 167: 24–31. [PubMed: 12406856]
65. Glass CK, and Ogawa S. 2006. Combinatorial roles of nuclear receptors in inflammation and immunity. Nat Rev Immunol 6: 44–55. [PubMed: 16493426]
66. Hou Y, Moreau F, and Chadee K. 2012. PPARgamma is an E3 ligase that induces the degradation of NFkappaB/p65. Nat Commun 3: 1300. [PubMed: 23250430]
67. Auphan N, DiDonato JA, Rosette C, Helmberg A, and Karin M. 1995. Immunosuppression by glucocorticoids: inhibition of NF-kappa B activity through induction of I kappa B synthesis. Science 270: 286–290. [PubMed: 7569976]
68. De Bosscher K, Vanden Berghe W, and Haegeman G. 2003. The interplay between the glucocorticoid receptor and nuclear factor-kappaB or activator protein-1: molecular mechanisms for gene repression. Endocr Rev 24: 488–522. [PubMed: 12920152]
69. Ding R, Sun X, Yi B, Liu W, Kazama K, Xu X, Deshpande DA, Liang C, and Sun J. 2021. Nur77 Attenuates Inflammasome Activation by Inhibiting Caspase-1 Expression in Pulmonary Vascular Endothelial Cells. Am J Respir Cell Mol Biol 65: 288–299. [PubMed: 33971110]
70. Hanna RN, Shaked I, Hubbeling HG, Punt JA, Wu R, Herrley E, Zaugg C, Pei H, Geissmann F, Ley K, and Hedrick CC 2012. NR4A1 (Nur77) deletion polarizes macrophages toward an inflammatory phenotype and increases atherosclerosis. Circ Res 110: 416–427. [PubMed: 22194622]
71. Kollmann TR, Levy O, Montgomery RR, and Goriely S. 2012. Innate immune function by Toll-like receptors: distinct responses in newborns and the elderly. Immunity 37: 771–783. [PubMed: 23159225]
72. Levy O. 2007. Innate immunity of the newborn: basic mechanisms and clinical correlates. Nature Reviews Immunology 7: 379–390.
73. PrabhuDas M, Adkins B, Gans H, King C, Levy O, Ramilo O, and Siegrist C-A 2011. Challenges in infant immunity: implications for responses to infection and vaccines. Nature immunology 12: 189–194. [PubMed: 21321588]

74. Gosselin D, Skola D, Coufal NG, Holtman IR, Schlachetzki JCM, Sajti E, Jaeger BN, O'Connor C, Fitzpatrick C, Pasillas MP, Pena M, Adair A, Gonda DD, Levy ML, Ransohoff RM, Gage FH, and Glass CK 2017. An environment-dependent transcriptional network specifies human microglia identity. Science 356.

75. Jones CV, Williams TM, Walker KA, Dickinson H, Sakkal S, Rumballe BA, Little MH, Jenkin G, and Ricardo SD 2013. M2 macrophage polarisation is associated with alveolar formation during postnatal lung development. Respir Res 14: 41. [PubMed: 23560845]

Key Points

Neonatal alveolar macrophages express a pro-inflammatory expression signature.

Neonatal and adult alveolar macrophages response similarly to inhaled LPS.

Unique features of alveolar macrophages are lost upon removal from the lung.

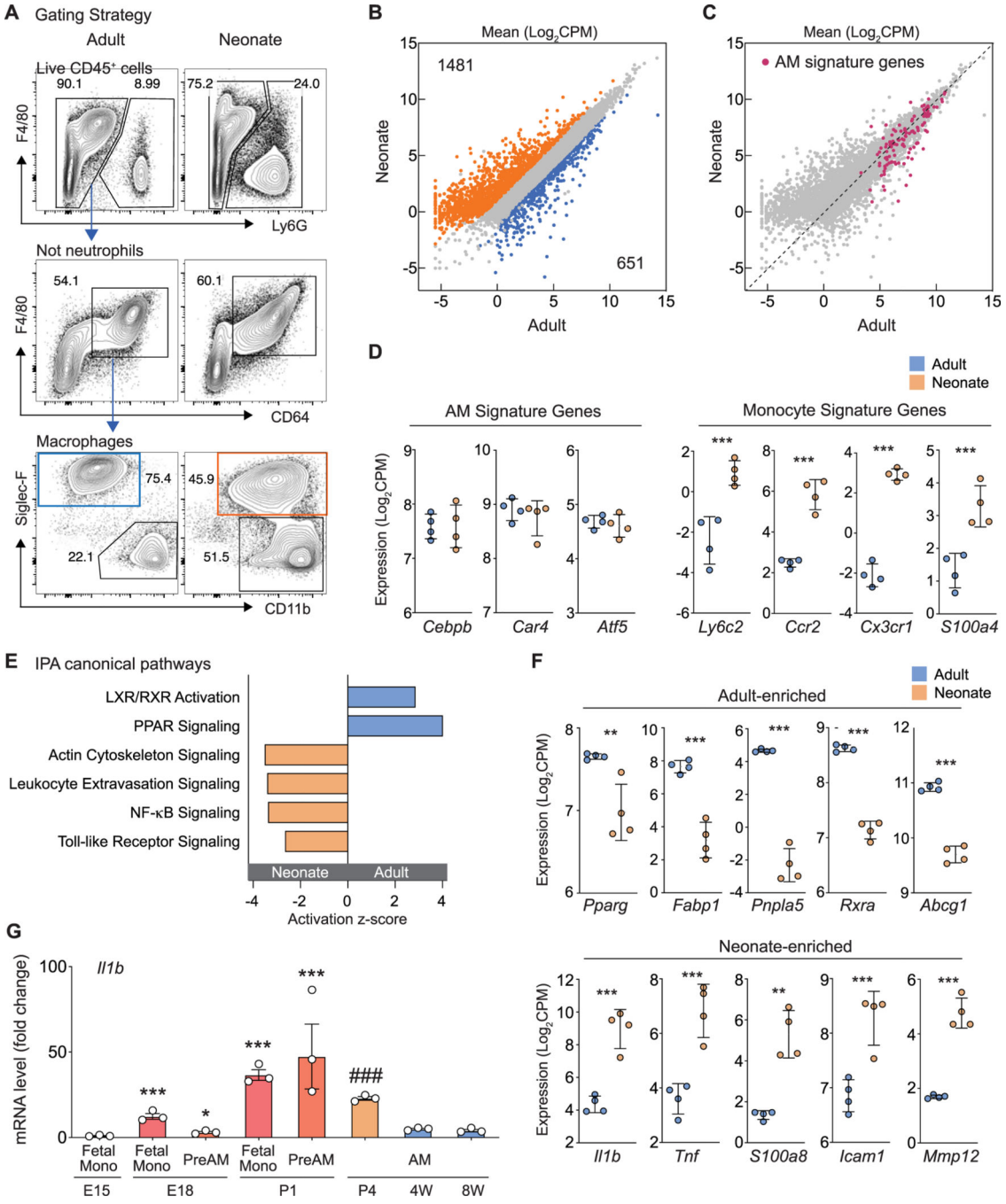

Figure 1. Distinct gene expression profiles of adult and neonatal AMs

(A) Flow cytometry analysis and gating strategy to identify AMs from adult and neonatal lungs. (B) Scatter plot of RNA-seq data comparing adult and neonatal AMs from control lungs. Data are from three independent experiments with n = 4 for each group. Color codes indicate differentially expressed genes ($Log_2FC > 1$, p-adj < 0.05) selected using limma. (C) Scatter plot of RNA-seq data comparing expression of AM signature genes (in red (41)) in both neonatal and adult AMs from control lungs. (D) Expression of AM signature genes and classical monocytes genes in adult and neonatal AMs. Asterisks represents statistical

significance calculated by limma: **p-adj < 0.01 and ***p-adj < 0.001. Error bars, SD. (E) IPA functional analysis of differentially expressed genes between adult and neonatal AMs. Bar graphs represent the activation z-score for a selection of highly significant pathways activated in adult AMs (positive z-score) and neonatal AMs (negative z-score). (F) Expression of indicated genes in adult and neonatal AMs. Asterisks represents statistical significance calculated by limma: **p-adj < 0.01 and ***p-adj < 0.001. Error bars, SD. (G) Real time PCR analysis *Il1b* mRNA expression in fetal monocyte, pre-AMs, or AMs. Data are represented as mean +/− SEM. Asterisks (*, compared to E15 fetal monocyte sample) and pound sign (#, compared to 8W adult sample) represent statistical significance calculated by unpaired t test using ΔC_T values: *p-adj < 0.05, ***p-adj < 0.001 and $^{###}$p-adj < 0.001. Data are from n=3 for each group.

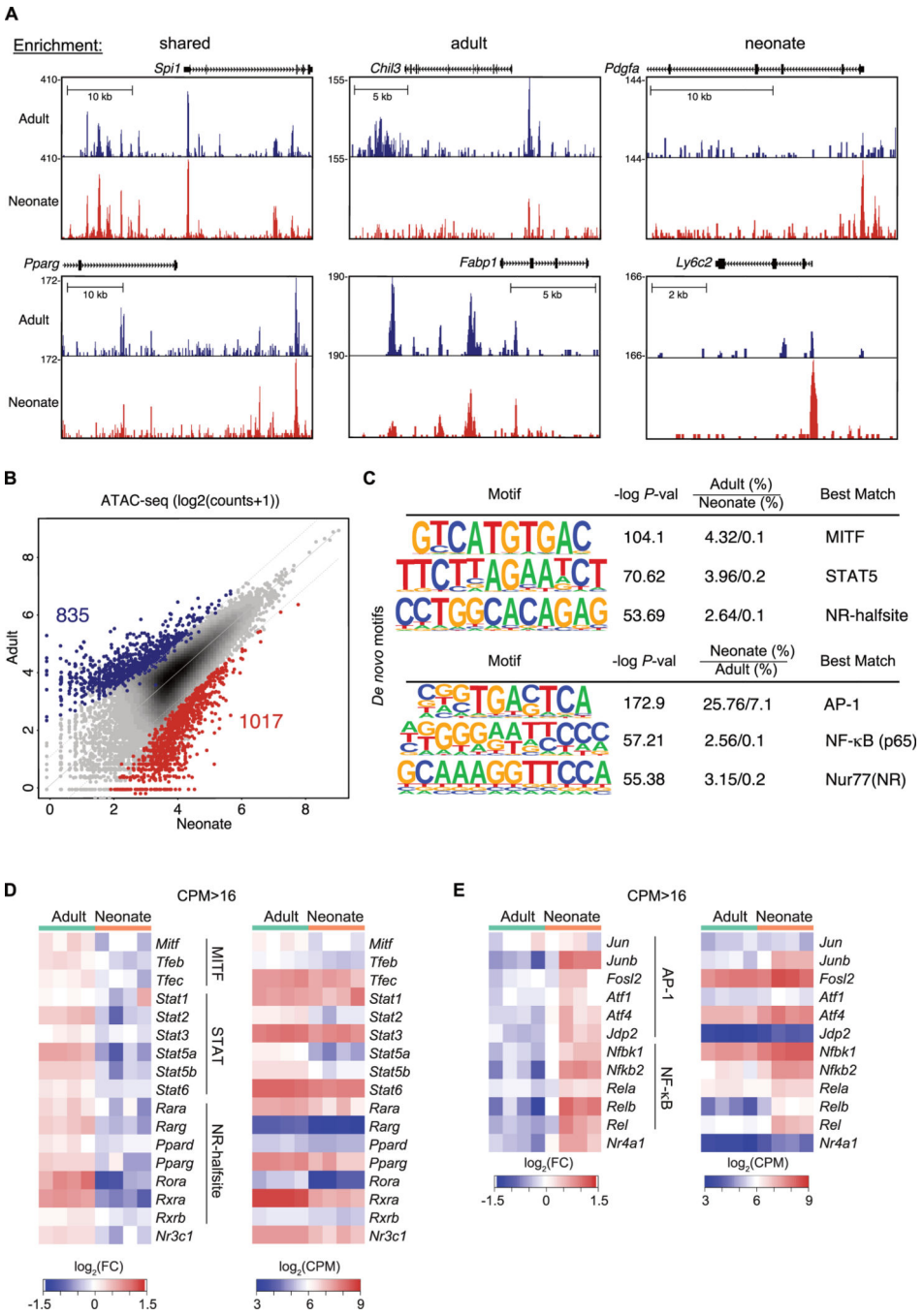

Figure 2. Unique epigenetic landscape of AMs from neonatal and adult lungs.

(A) UCSC genome browser tracks of ATAC-seq peaks in the vicinities of indicated genes in AMs. (B) Scatterplot comparing distal ATAC-seq peak tag counts (distance from TSS > 2kb) between neonatal and adult AMs. Color codes indicate differential chromatin regions ($Log_2FC > 1$, p-adj < 0.05). Data shown here are IDR peaks for each group. Two independent replicates were performed for both neonatal and adult cells. (C) Homer *de novo* motif enrichment analysis (39) of distal open chromatin regions specific to either adult or neonatal AMs. (D, E) Heatmap of highly expressed TF family members (CPM > 16 in at

least one sample) corresponding to motifs identified in Figure 2C and Supplemental Figure S1C.

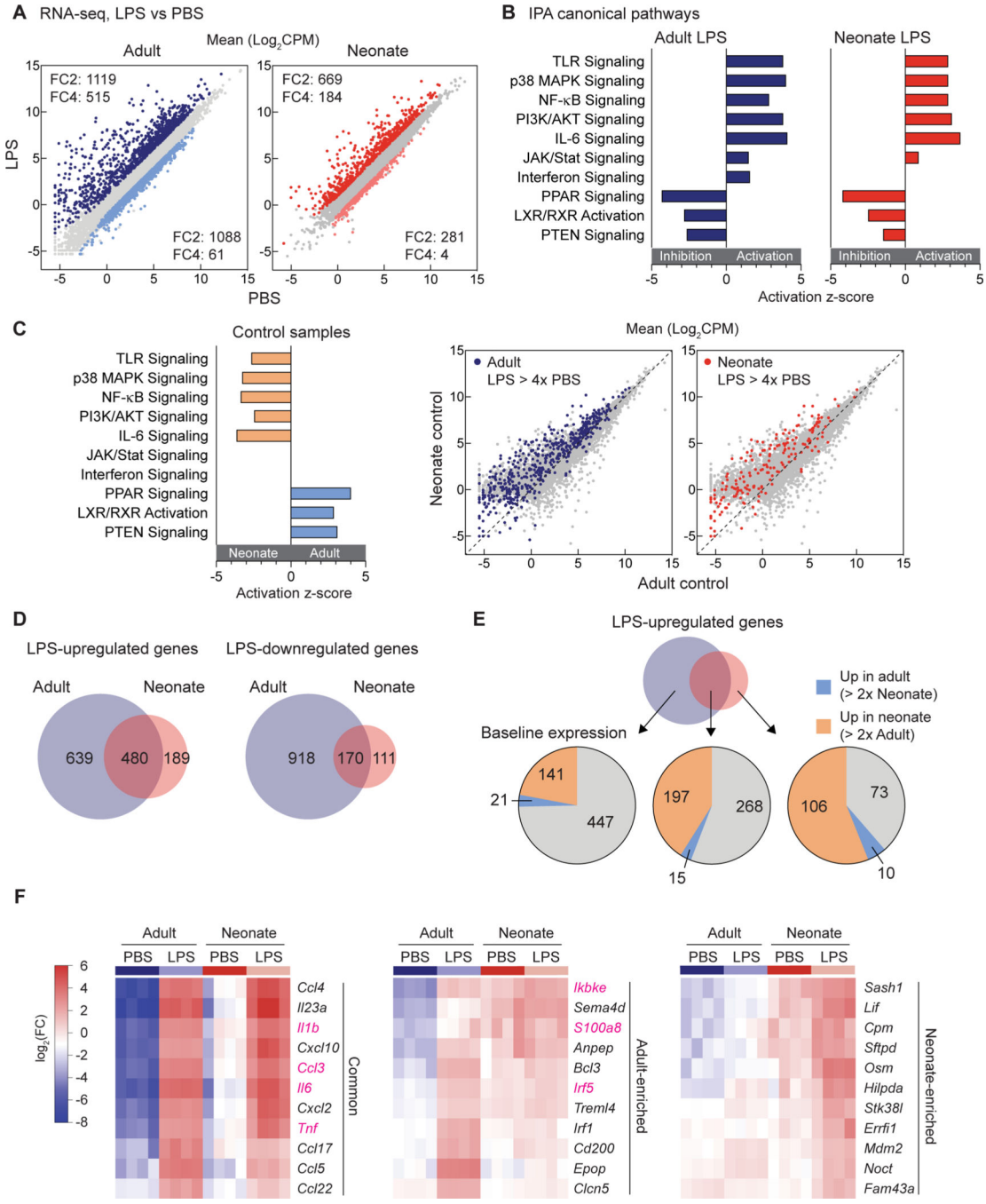

Figure 3. Neonatal AMs express higher baseline levels of LPS-induced transcripts.

(A) Scatter plot of RNA-seq data comparing gene expression between AMs isolated after 2h of instillation with LPS or PBS (control). Data are from three independent experiments with n = 4 for each group. Color codes indicate differentially expressed genes ($Log_2FC > 1$, p-adj < 0.05) selected using limma. (B) IPA functional analysis of differentially expressed genes ($Log_2FC > 1$, p-adj < 0.05) between LPS and PBS samples. Bar graphs represent the activation z-score for a selection of highly significant pathways activated (positive z-score) or inhibited (negative z-score) following LPS activation. (C) Bar graph on the left panel

compares z-scores for indicated pathways from Figure 3B in adult (positive z-score) and neonatal AMs (negative z-score) under control conditions. Scatter plots on the right show RNA-seq data from adult and neonatal AMs under control conditions. Genes upregulated following LPS instillation are color-coded. Data are from three independent experiments with n = 4 for each group. (D) Venn diagram of upregulated and downregulated genes 2h following intranasal LPS instillation in adult AMs vs neonatal AMs. (E) Pie chart depicting the relative baseline expression of genes upregulated after LPS instillation in adult and neonatal AMs. (F) Heat map of representative LPS upregulated genes in both adult and neonatal AMs (common), primarily in adult AMs (adult-enriched), or primarily in neonatal AMs (neonate-enriched). CPM > 16 in at least one sample.

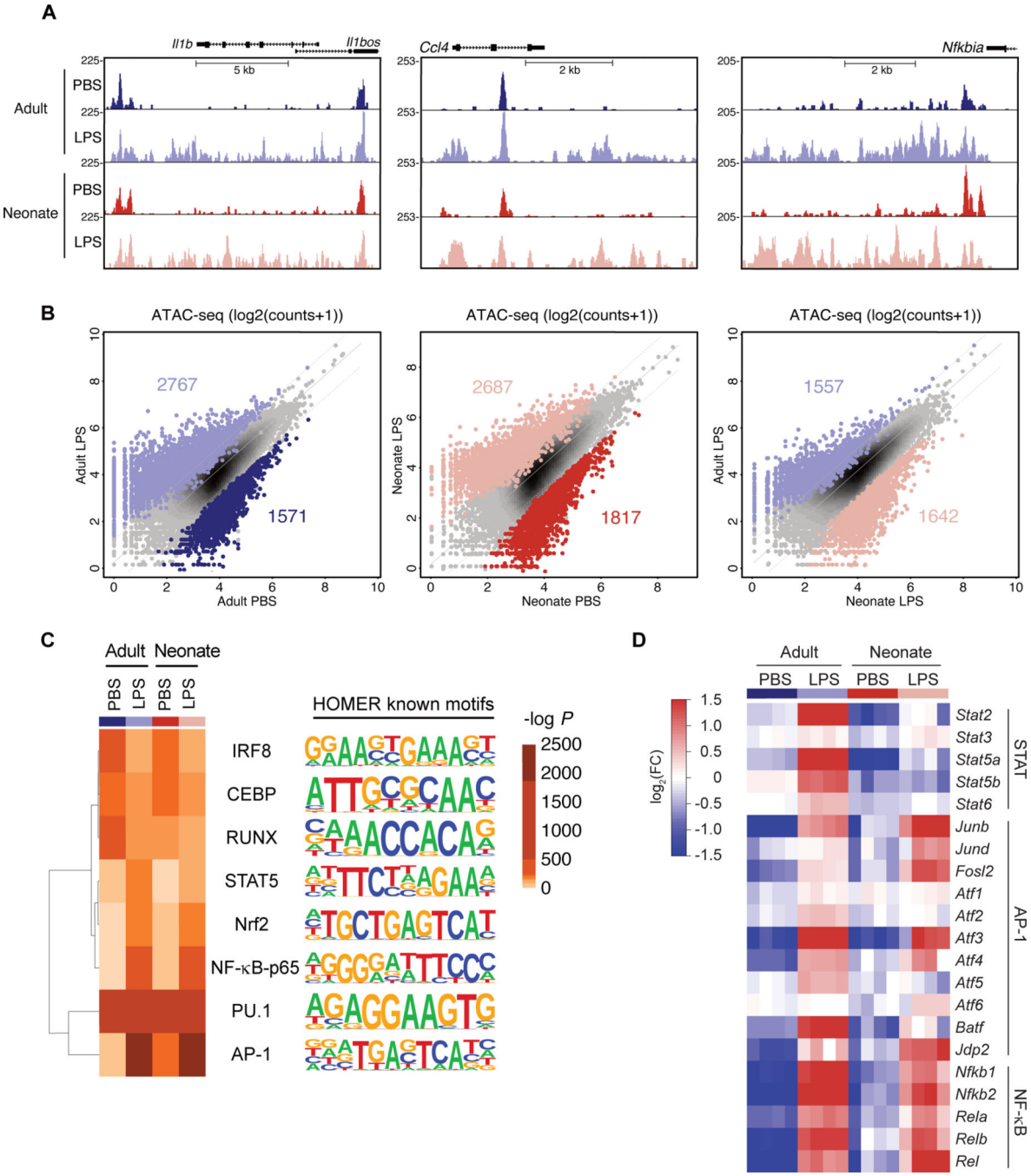

Figure 4. Effects of LPS on AM chromatin landscape in vivo.

(A) UCSC genome browser tracks of ATAC-seq peaks in the vicinities of activated genes following intranasal LPS instillation in adult and neonatal AMs. (B) Scatterplot comparing distal ATAC-seq peak tag counts (distance from TSS > 2kb) between PBS and LPS samples (left and middle) and LPS samples of adult and neonatal AMs (right). Color codes indicate differential chromatin regions ($Log_2FC > 1$, p-adj < 0.05). Data shown here are IDR peaks from each group. Two independent replicates were performed for each sample. (C) Known motifs enriched at distal open chromatin regions following LPS instillation in adult and

neonatal AMs. (D) Heatmap of highly expressed TF family members (CPM > 16 in at least one sample) predicted to bind STAT, AP-1, and NF-κB motifs.

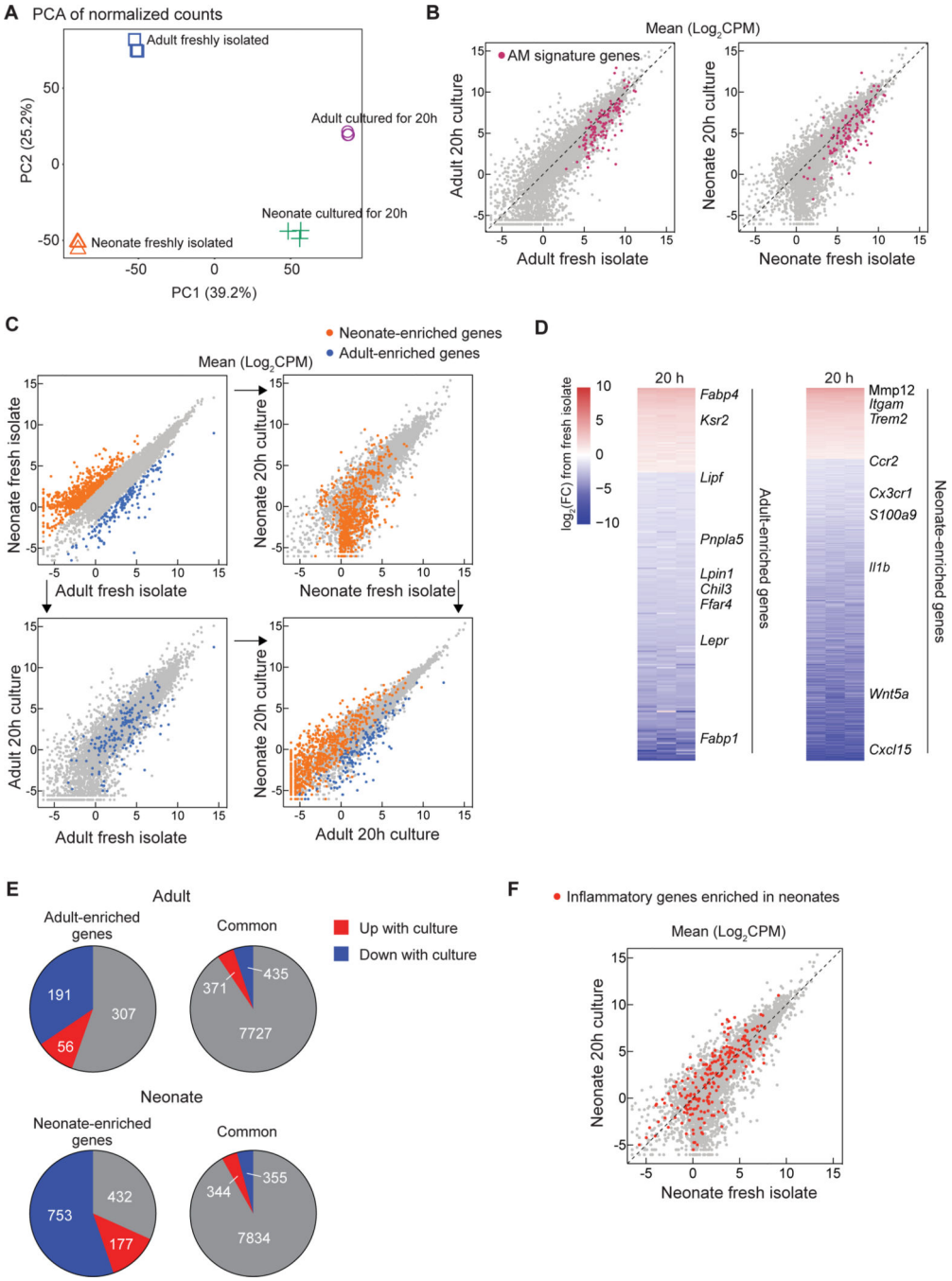

Figure 5. The lung microenvironment impacts gene expression in adult and neonatal AMs.

(A) PCA of the 12,149 detectable genes in freshly isolated adult and neonatal AMs and after maintenance in culture for 20 h. Two independent cell isolations and FACS sorts were used to generate 3 replicates for each time point and condition. (B) Scatter plot of RNA-seq data comparing freshly isolated AMs with AMs cultured for 20 h. AM signature genes (41) are shown in red. (C) Scatter plot of RNA-seq data illustrating the impact of removal from the lung microenvironment on expression of genes differentially expressed in neonatal (orange) and adult (blue) AMs ($Log_2FC > 2$, p-adj < 0.05; n = 3). (D) Heatmap illustrating

changes in adult- and neonatal-enriched gene expression following ex vivo culture. (E) Pie chart depicting effects of culture environment on (top) adult-enriched ($Log_2FC > 1$, p-adj < 0.05) or commonly expressed genes ($Log_2FC < +/- 0.5$, p-adj < 0.05) or (bottom) neonatal-enriched or commonly expressed genes. (F) Scatter plot of RNA-seq data comparing freshly isolated neonatal AMs with cultured neonatal AMs. Genes upregulated in neonatal AMs by in vivo LPS exposure are indicated in red.

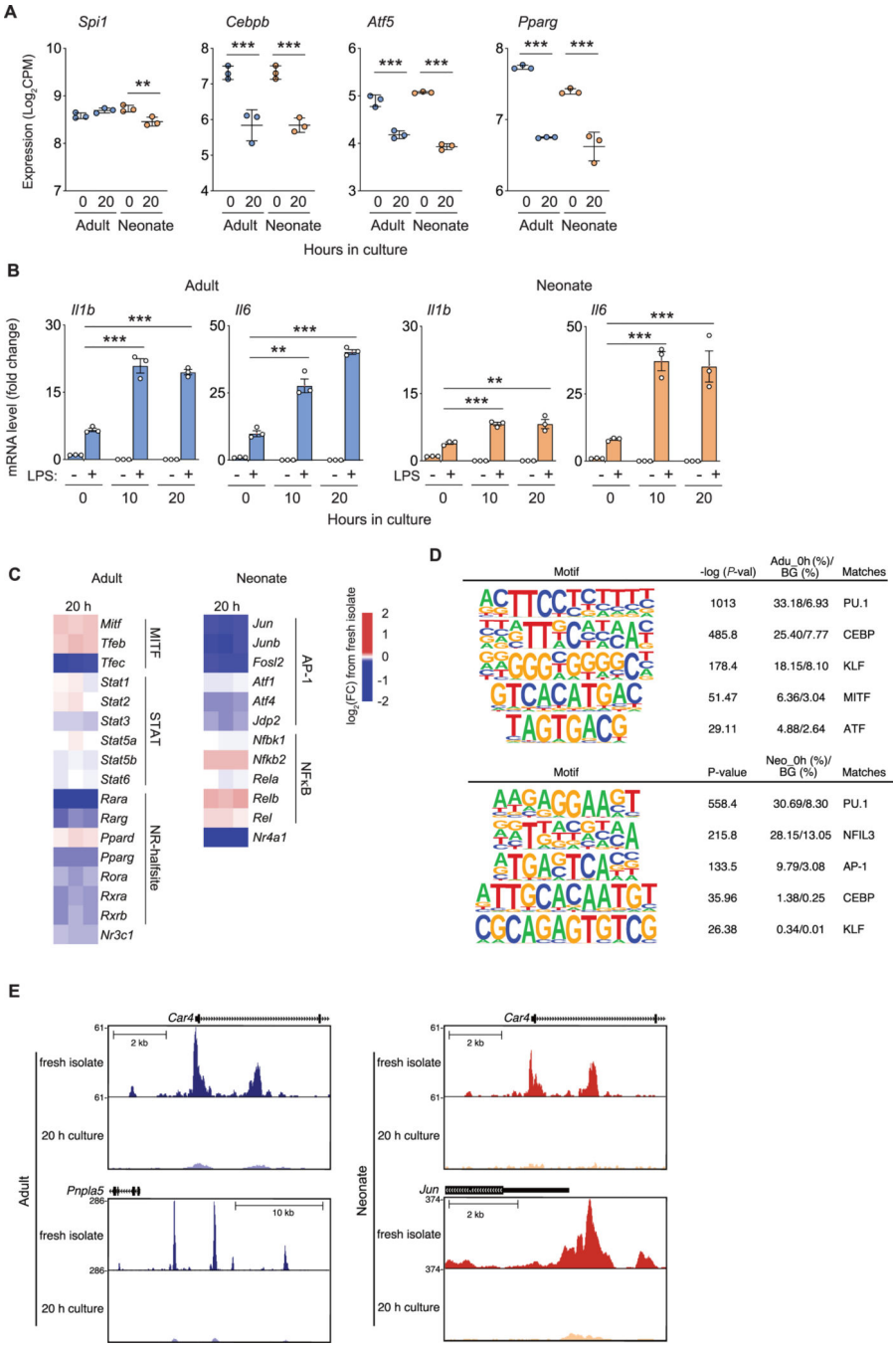

Figure 6. The influence of lung microenvironment on innate immune response and chromatin landscapes in adult and neonatal AMs.

(A) RNAseq expression of TFs important for macrophage development in freshly isolated and cultured AMs. Two independent cell isolations and FACS sorts were used to generate 3 replicates for each time point and condition. Asterisks represents statistical significance calculated by limma: **p-adj < 0.01 and ***p-adj < 0.001. Error bars, +/− SD. (B) Real time PCR measurement of *Il1b* and *Il6* mRNA expression in adult and neonatal AMs treated with LPS (2 h exposure) either immediately after isolation from the lung or following 10–20 h of ex vivo culture. Data are represented as mean +/− SEM. Asterisks represents statistical

significance calculated by unpaired t test using ΔC_T values: **p-adj < 0.01 and ***p-adj < 0.001. N = 3 for each group. (C) Heatmap illustrating the effect of culture environment on expression of TF family members (16 > CPM in at least one sample) identified in Figure 2C and Supplemental Figure S1C. (D) Homer *de novo* motif enrichment analysis of distal open chromatin regions associated with genes that exhibit reduced expression after ex vivo culture. (E) UCSC genome browser tracks displaying impact of ex vivo culture on the ATAC-seq peaks in the vicinities of selected genes in freshly isolated and cultured AMs.